Supplementary Materials

Metallic and highly conducting two-dimensional atomic arrays of sulphur enabled by molybdenum disulfide nanotemplate

This PDF file includes:
Supplementary Figure 1 to 21
Discussions on interpretation of computational results

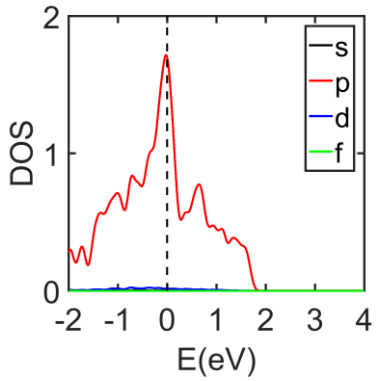

Supplementary Figure 1. Density of States (DOS) plot for different orbitals of S atoms arranged in a triangular array with inter-atomic spacing of 0.32 nm.

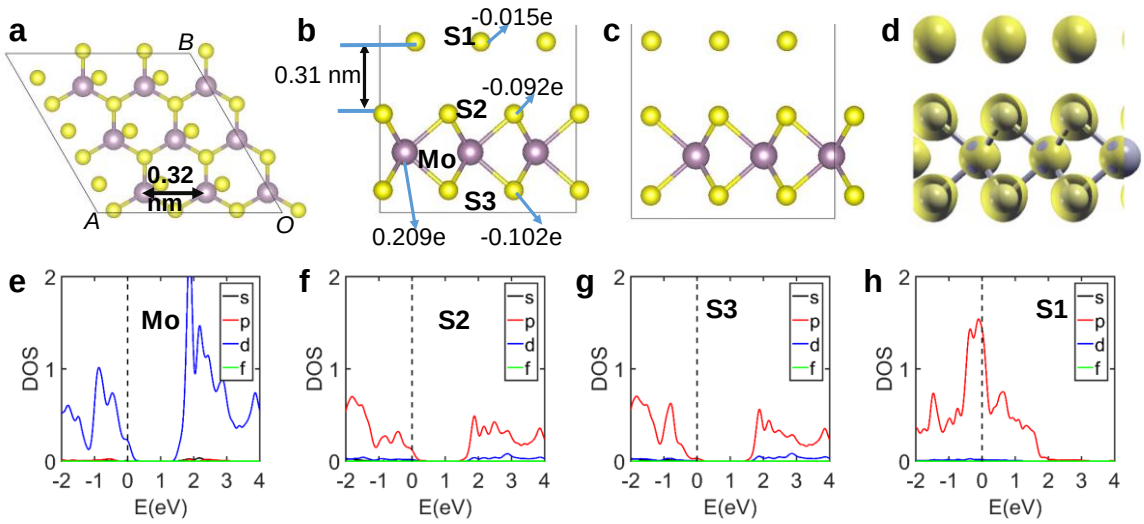

Supplementary Figure 2. (a) Top view of triangular array of S atoms on monolayer 2H-MoS_2. The Mo-Mo in-plane spacing is 0.32 nm. OA, OB are other two viewing directions. (b) OA view of triangular array of S atoms on monolayer 2H-MoS_2. The Hirshfeld charges are labeled for each type of atom. The vertical distance between S1 and S2 atom determined from structure relaxation is 0.31 nm. (c) OB view of triangular array of S atoms on monolayer 2H-MoS_2. (d) Charge density isosurface plot (isosurface value 0.09 electrons /bohr^3). (e) Density of States (DOS) plot for different orbitals of Mo atoms. (f) DOS plot for different orbitals of S2 atoms. (g) DOS plot for different orbitals of S3 atoms. (h) DOS plot for different orbitals of S1 atoms.

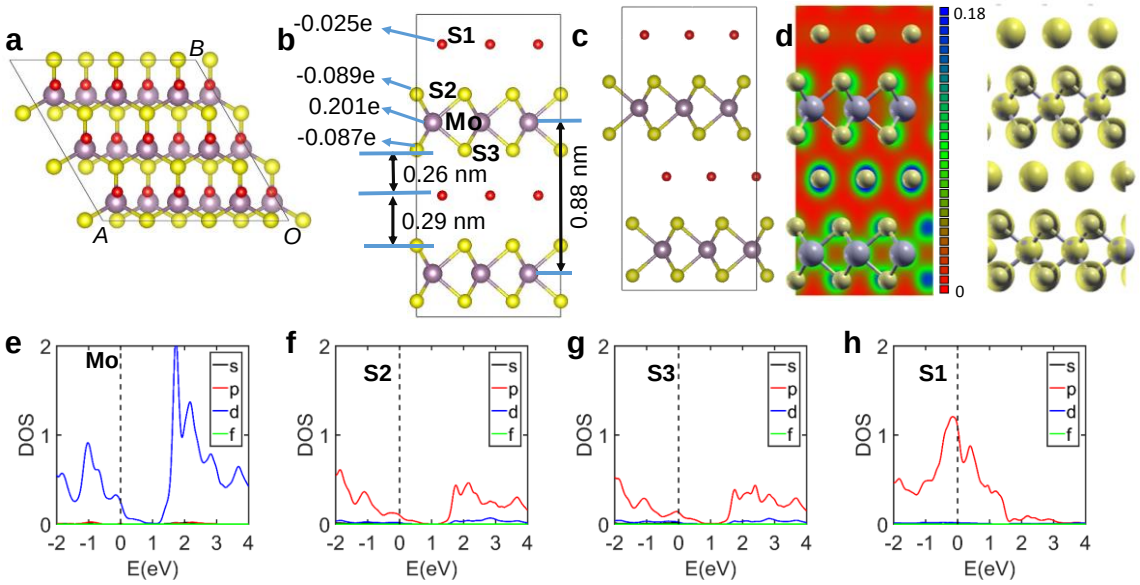

Supplementary Figure 3. (a) Top view of triangular array of S atoms intercalated in layered 2H-MoS_2. The Mo-Mo in-plane spacing is 0.32 nm. OA, OB are other two viewing directions. (b) OA view of triangular array of S atoms intercalated in layered 2H-MoS_2. Several representative interlayer distances are determined from structure relaxation and labeled. The Hirshfeld charges are labeled for each type of atom. (c) OB view of triangular array of S atoms intercalated in layered 2H-MoS_2. (d) Charge density 2D contour plot (colored range: 0 to 0.18 electrons/bohr^3) on a plane perpendicular to OA view direction and charge density isosurface plot (isosurface value 0.09 electrons /bohr^3) along OB view. (e) Density of States (DOS) plot for different orbitals of Mo atoms. (f) DOS plot for different orbitals of S2 atoms. (g) DOS plot for different orbitals of S3 atoms. (h) DOS plot for different orbitals of S1 atoms.

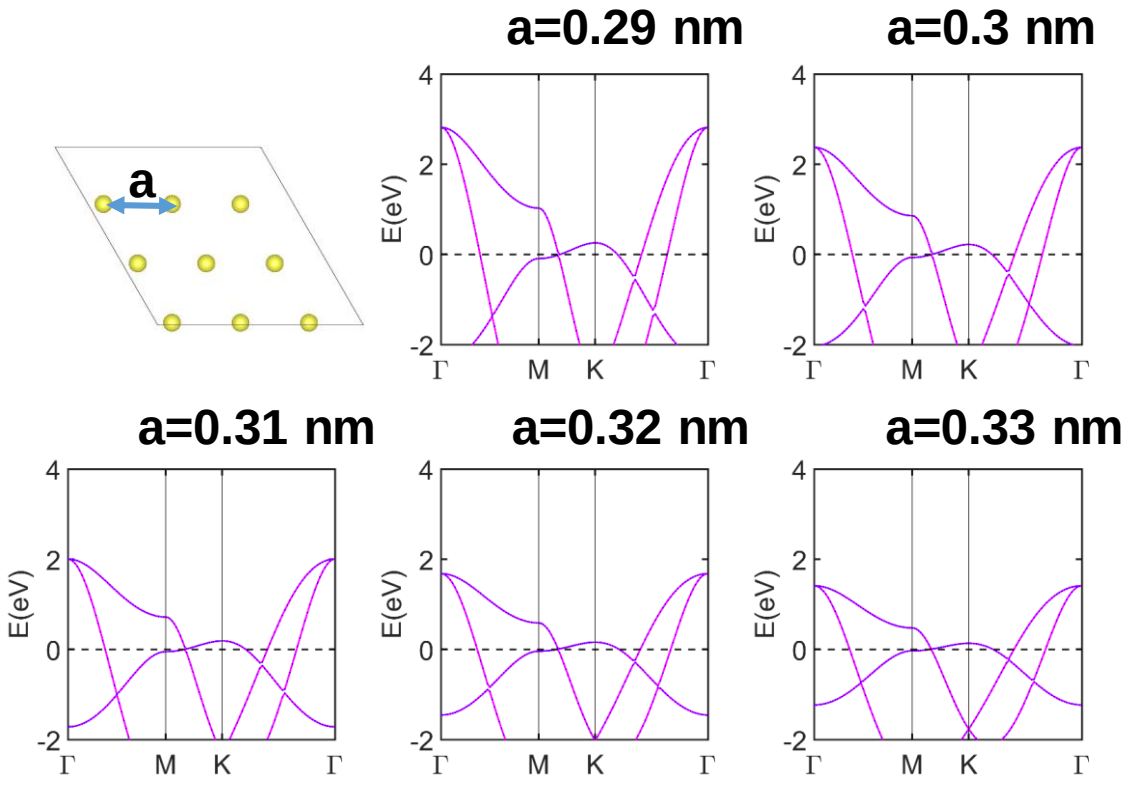

Supplementary Figure 4. Band structures of an array of triangularly patterned S atoms for a variety of inter-atomic spacings.

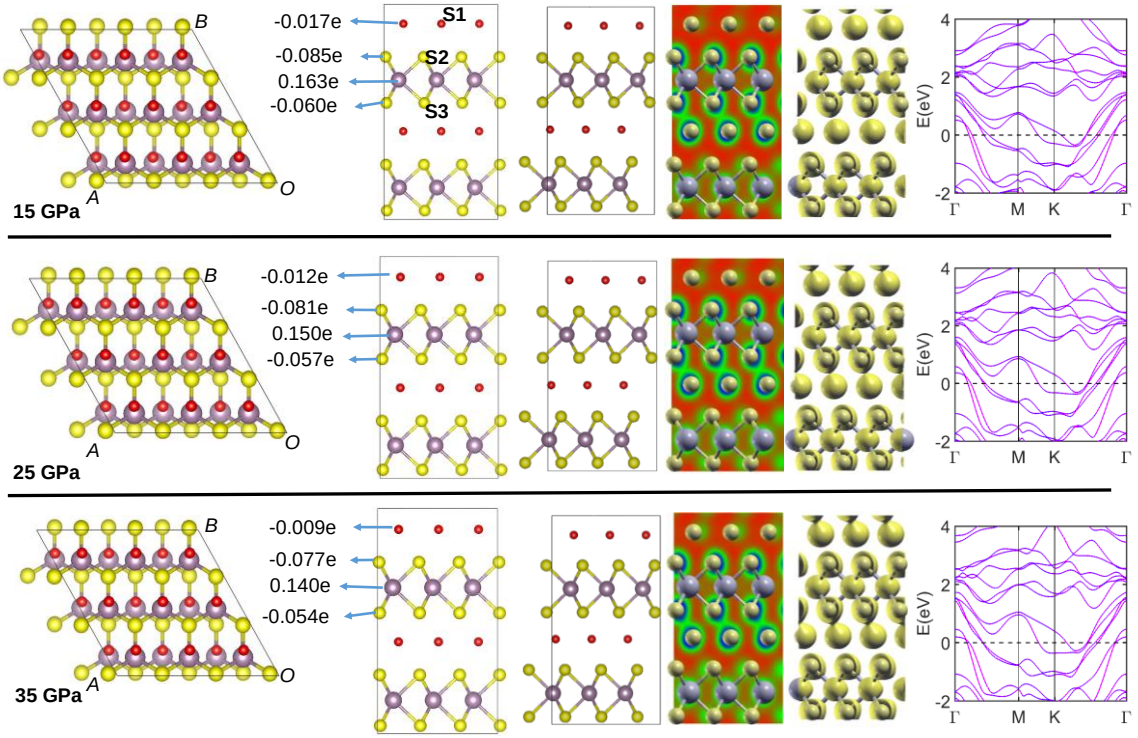

Supplementary Figure 5. Top view, OA view, OB view, charge density 2D contour plot (colored range: 0 to 0.18 electrons/bohr^3, see color bar in Supplementary Figure 3) on a plane perpendicular to OA view direction, charge density isosurface plot (isosurface value 0.09 electrons /bohr^3) and band structure of layered 2H-MoS_2-S at 15 GPa, 25 GPa and 35 GPa. The Hirshfeld charges are labeled for each type of atom.

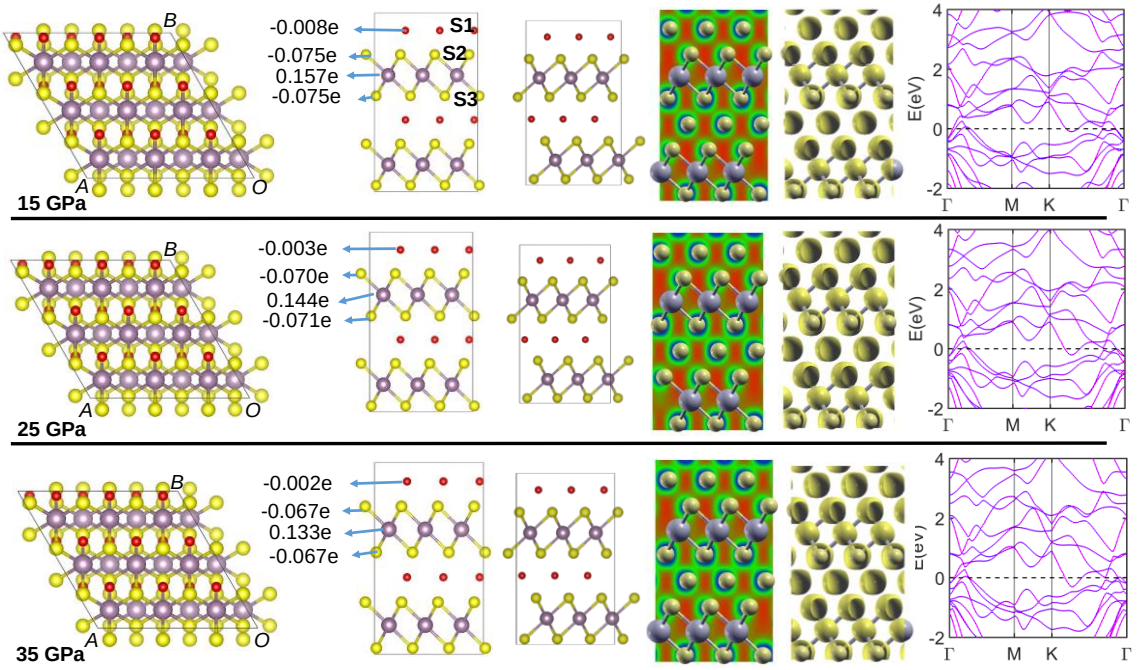

Supplementary Figure 6. Top view, OA view, OB view, charge density 2D contour plot (colored range: 0 to 0.18 electrons/bohr^3, see color bar in Supplementary Figure 3) on a

plane perpendicular to OA view direction, charge density isosurface plot (isosurface value 0.09 electrons /bohr^3) and band structure of layered 1T-MoS_2-S at 15 GPa, 25 GPa and 35 GPa. The Hirshfeld charges are labeled for each type of atom.

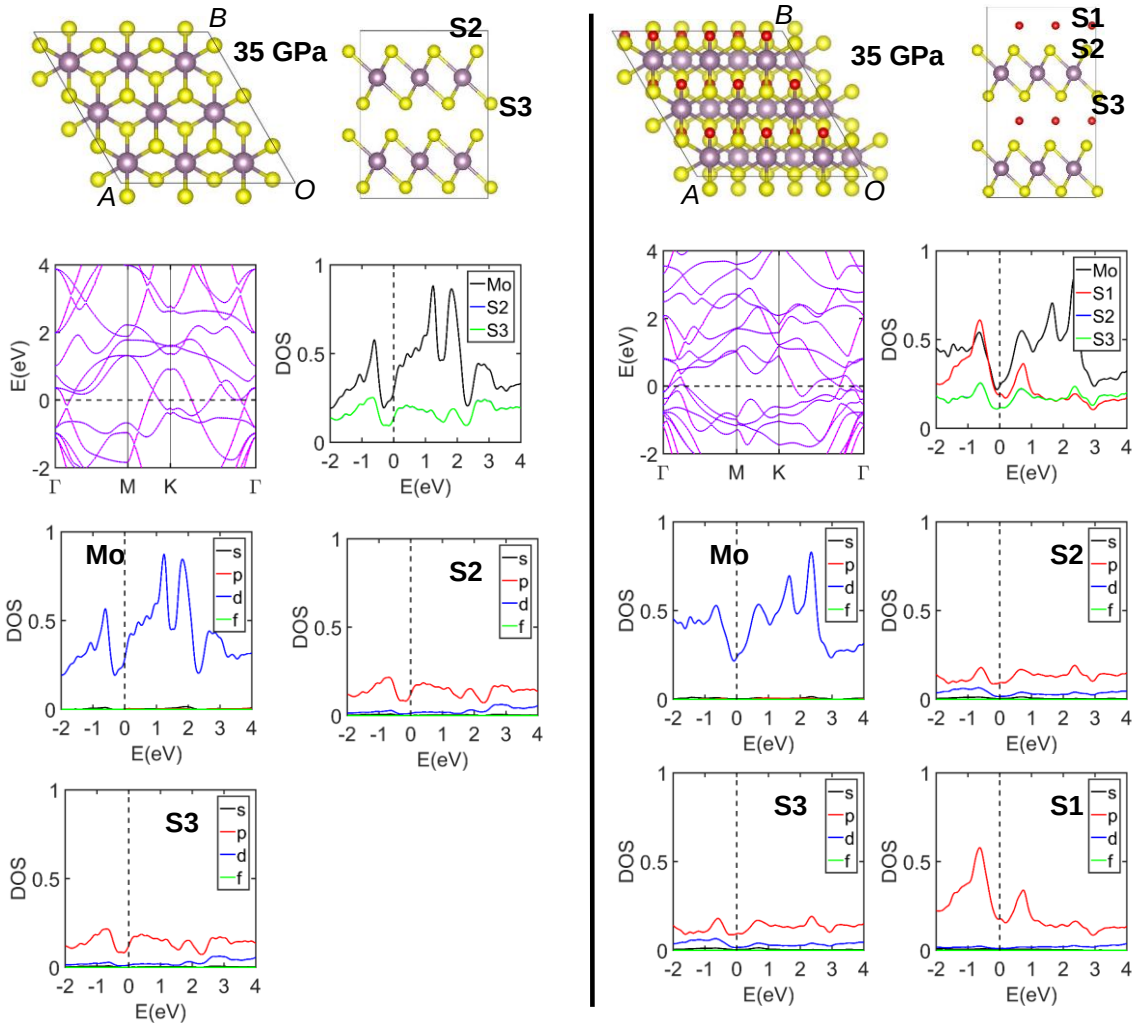

Supplementary Figure 7. Left: DOS and band structure of layered 1T-MoS_2 at 35 GPa. Right: DOS and band structure of layered 1T-MoS_2-S at 35 GPa.

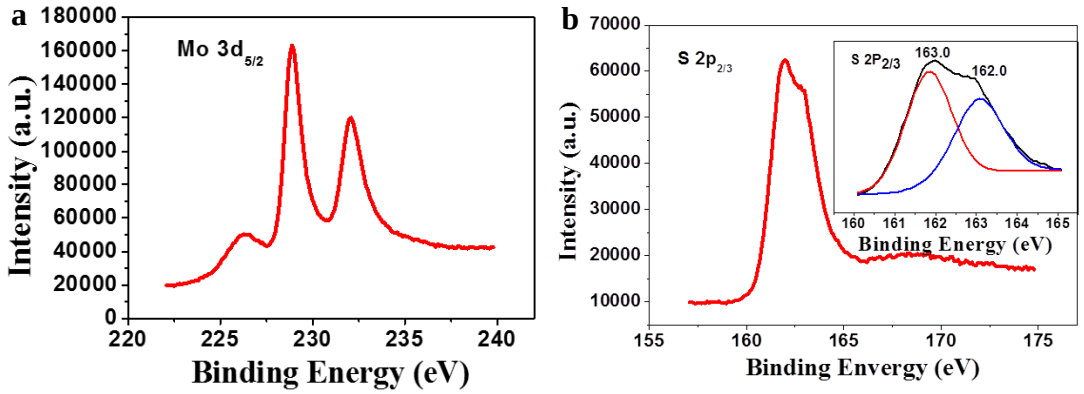

Supplementary Figure 8. XPS spectra of conducting MoS_2-S. (a) The Mo 3d spectrum. (b) S 2p spectrum. The inset shows two doublets with S 2p2/3 energies of 162.0 and 163.0. The ratio of these doublets is close to 5:4.

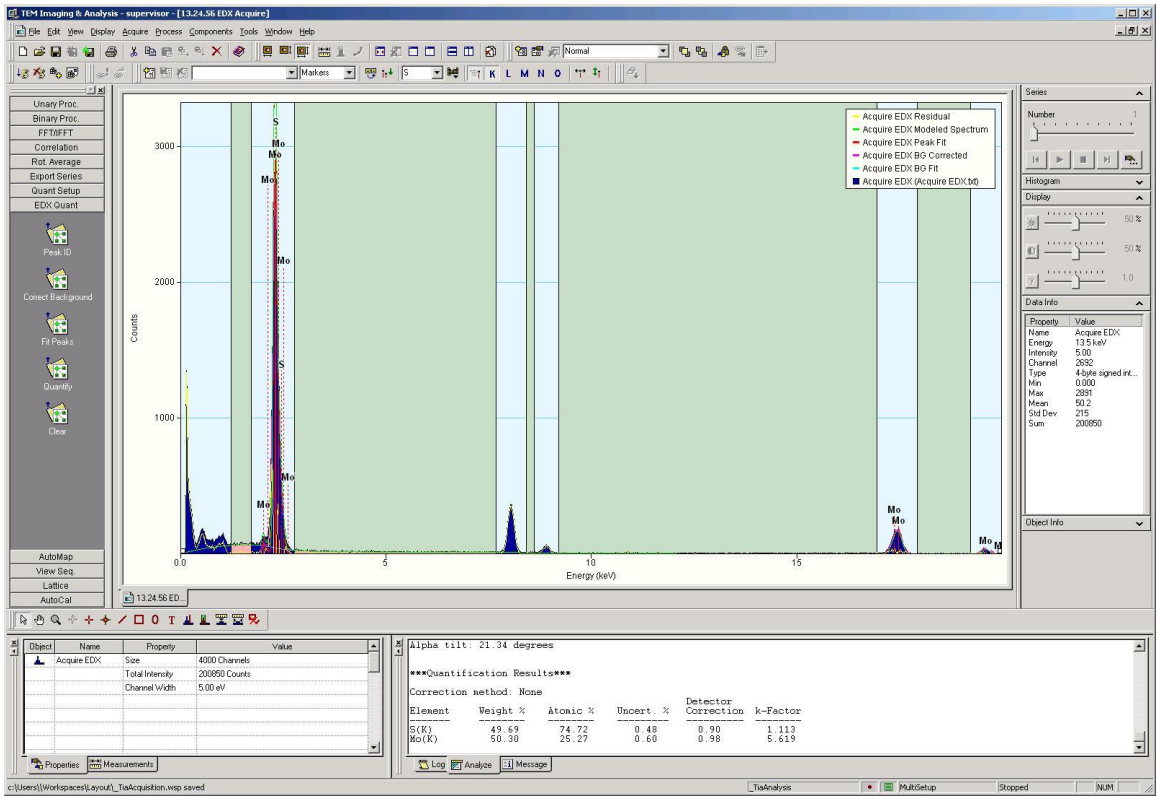

Supplementary Figure 9. EDX of TEM of conducting MoS_2-S

Supplementary Figure 10. clear “Huskies” picture could be reflected on MoS_2-S film.

Supplementary Figure 11. Uniform colloidal dispersion in water.

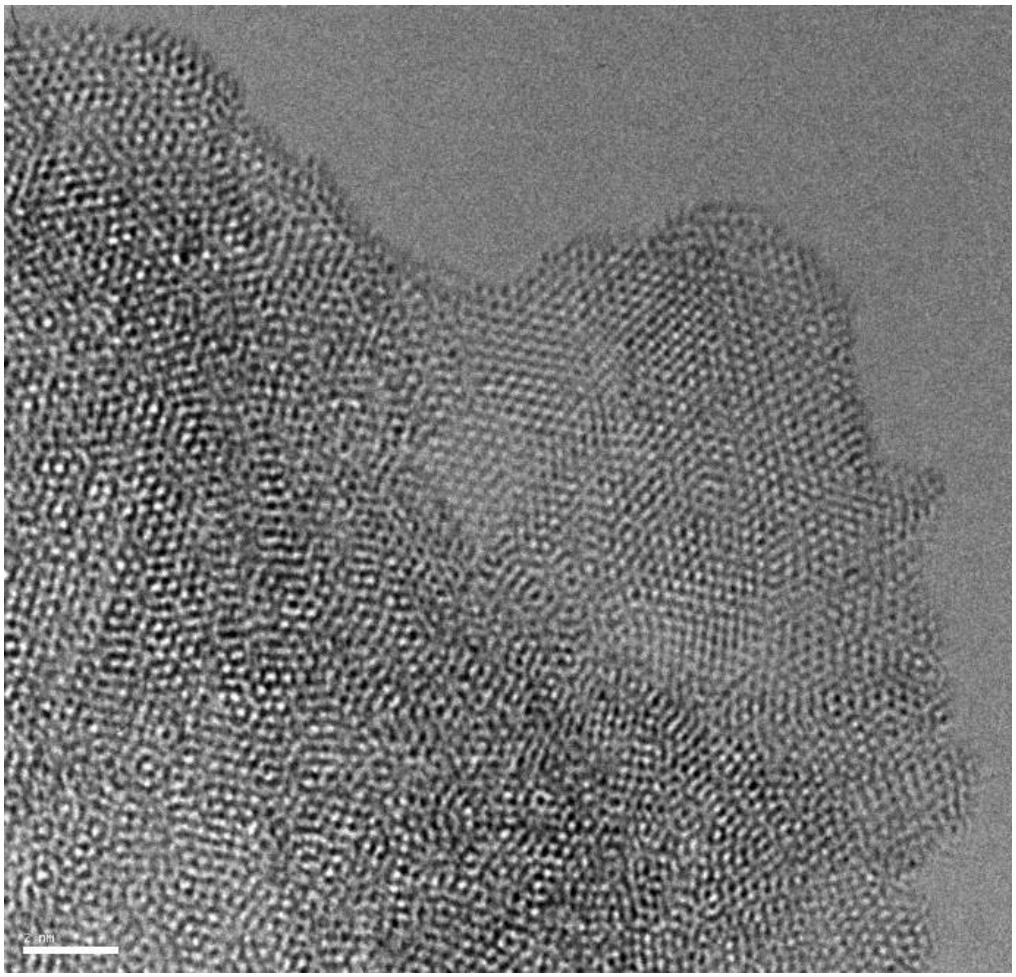

Supplementary Figure 12. Atomic resolution TEM images (Scale bar: 2 nm)

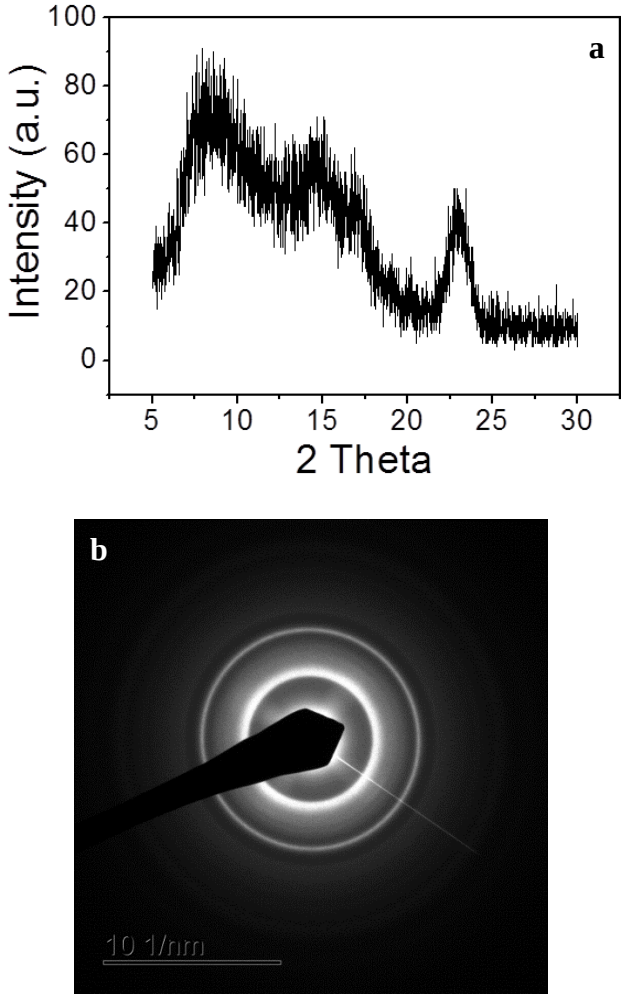

Supplementary Figure 13. Characterization of structure of MoS_2-S. (a) XRD pattern of MoS_2-S. (b) SAED obtained from HRTEM.

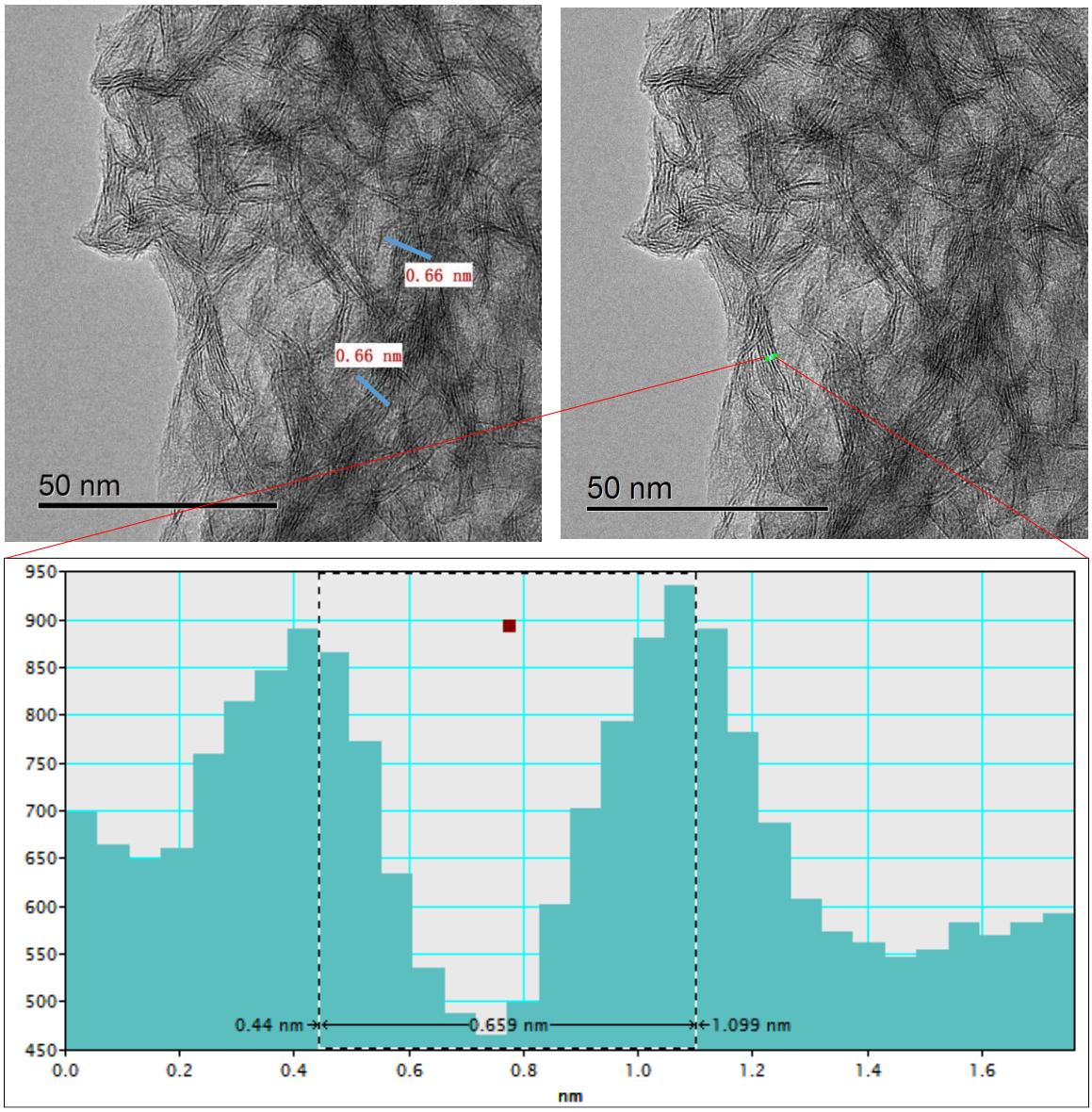

Supplementary Figure 14. Layer distance measurement on as-prepared MoS_2-S

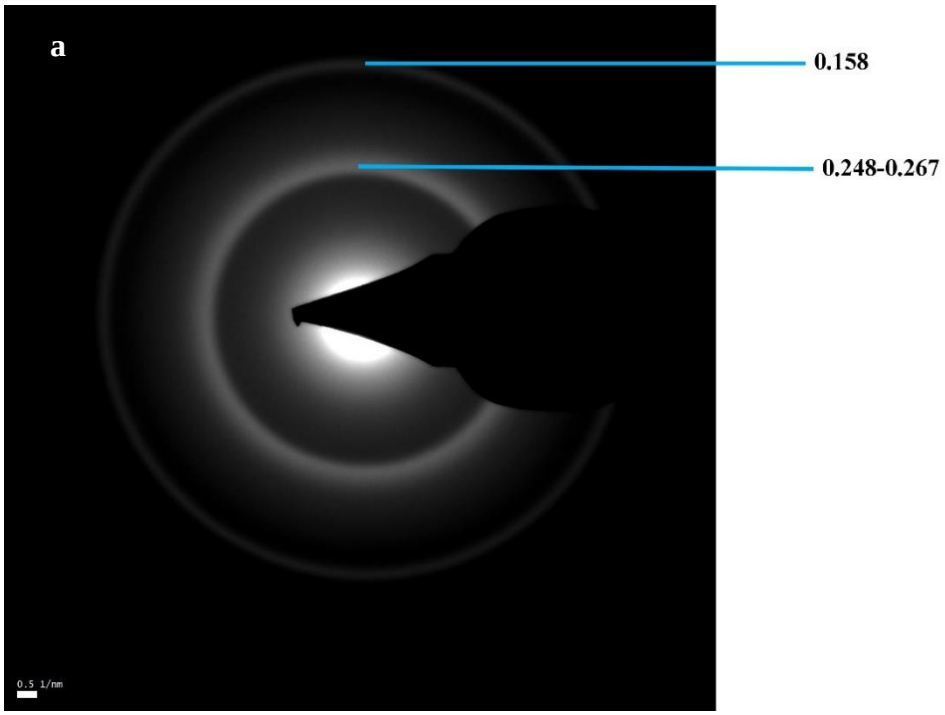

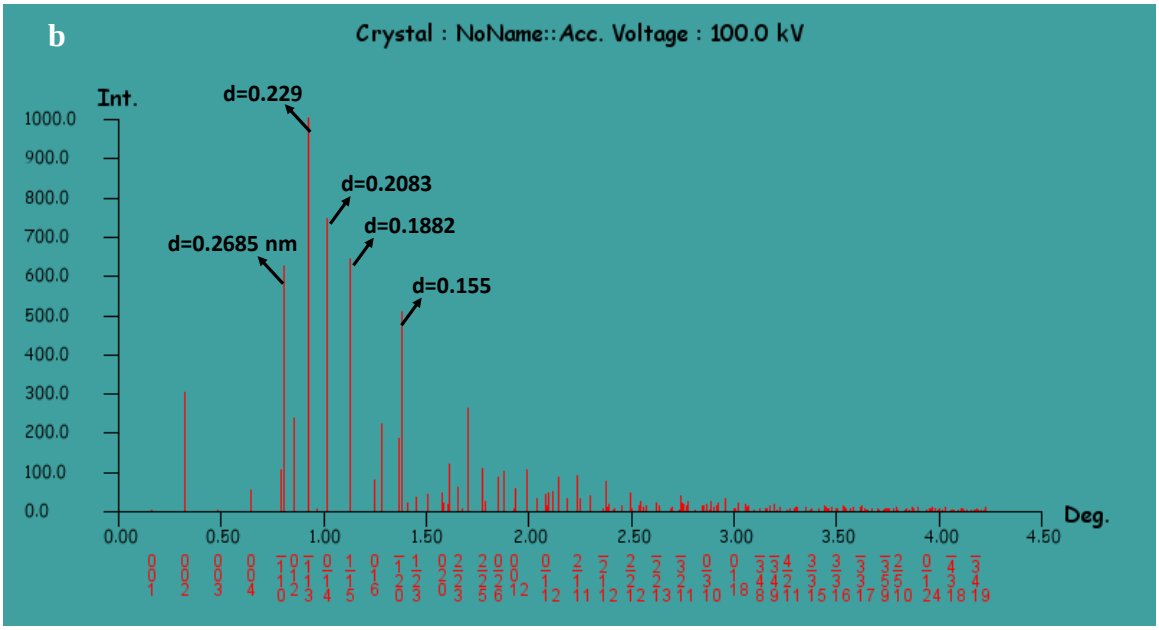

Supplementary Figure 15. (a) SAED (b) Raw calculated diffraction pattern of a 2H-MoS_2-S structure.

Supplementary Figure 15 (b) is calculated for the following 2H-MoS_2-S structure

Lattice parameters:

a=b=0.31 nm, c=1.32 nm, alpha=beta=90 degree, gamma=120 degree.

Atomic fractional coordinates:

Mo	0.89670	0.33598	0.15538
S	0.23560	0.01378	0.27356
S	0.23010	0.00149	0.03705
S	0.98874	0.52781	0.40811
Mo	0.38911	0.33822	0.65576
S	0.72838	0.01676	0.77402
S	0.72066	0.00261	0.53735
S	0.49164	0.53489	0.90803

EMS software from Stadelman is used to calculate the diffraction pattern. The structure contains crystallographic planes (h, k, l) with lattice parameters defined by a,b,c as described above. We can calculate the lattice spacing d(h, k, l) for all (h, k, l) planes of the structure. We also calculate the structure factor for all (h, k, l) planes. If the structure factor of a reflection (h, k, l) is zero or weak, then the plane (h, k, l) will not be visible in diffraction or image. The vertical axis of Supplementary Figure 15(b) is representing the number that is directly proportional the structure factor. The zero on horizontal axis corresponds the position of transmitted beam in diffraction pattern and as we go away from it the location of the peaks indicate the radius of the rings we see in diffraction.

Supplementary Figure 15(b) shows that it has nice peaks at plane spacing 0.2685 nm, 0.229 nm, 0.2083 nm, and 0.1882 nm respectively. It also has nice peaks at 0.155 nm. Since our simulation is essentially for bulk structure but our experimental sample only has a few layers, we have decided to ignore the out-of-plane components by only considering plane (h, k, 0). As a result, the peaks on 0.229 nm and 0.2083 nm and 0.1882 nm are not plotted in main text figure 4h. The peak 0.2685 nm and 0.155 nm fit very well with SAED in Supplementary Figure 15(a).

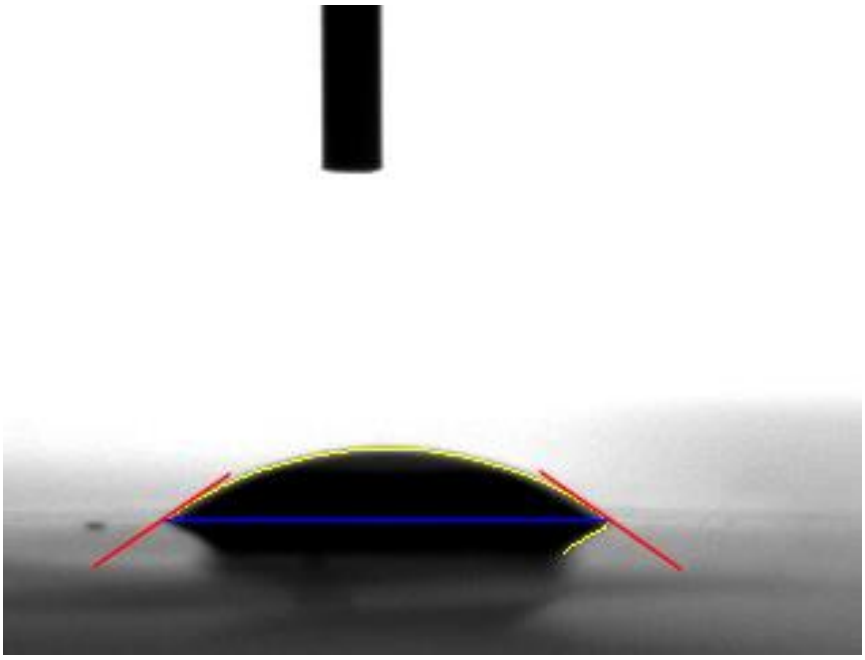

Supplementary Figure 16. Contact angle measurement of MoS_2-S. The contact angle between water and MoS_2-S film was measured by drop casting a droplet of water from a manually controlled syringe system (Phoenix 150) onto the film. The angles obtained right after drop casting and after a duration of 20 minutes are 61.8, 34.8 respectively, indicating the hydrophilic nature of MoS_2-S film.

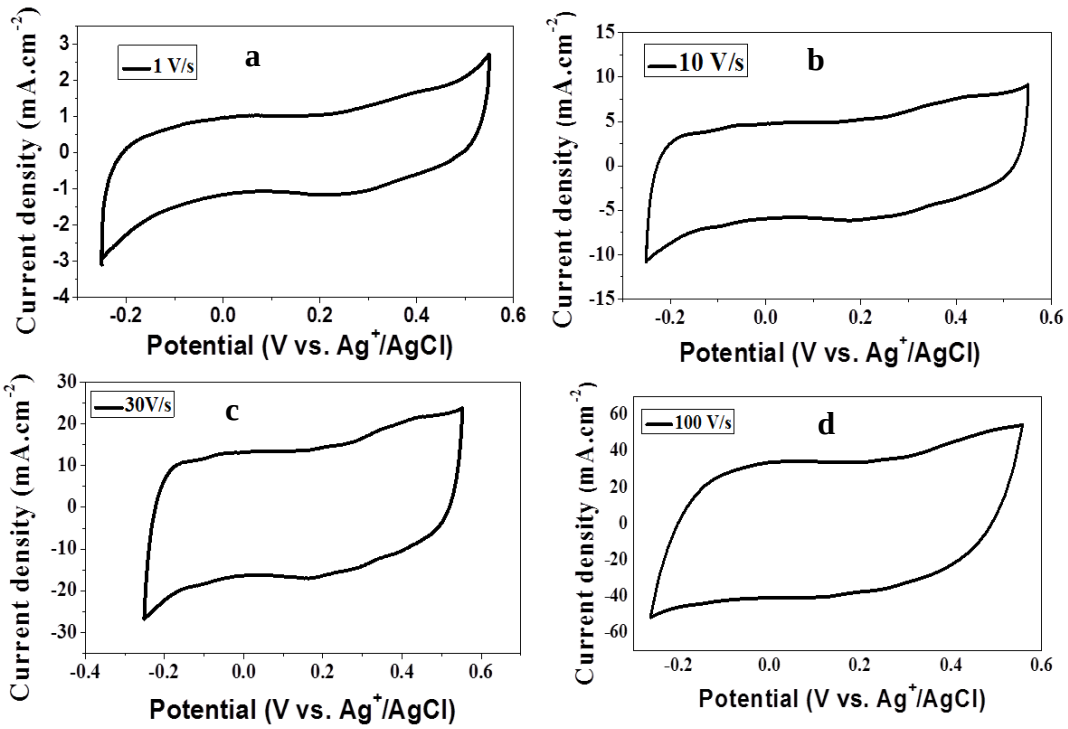

Supplementary Figure 17. CV of ultrahigh scan rates of MoS_2-S in H_2SO_4. (a) 1V/s, (b) 10V/s, (c) 30V/s, (d) 100V/s

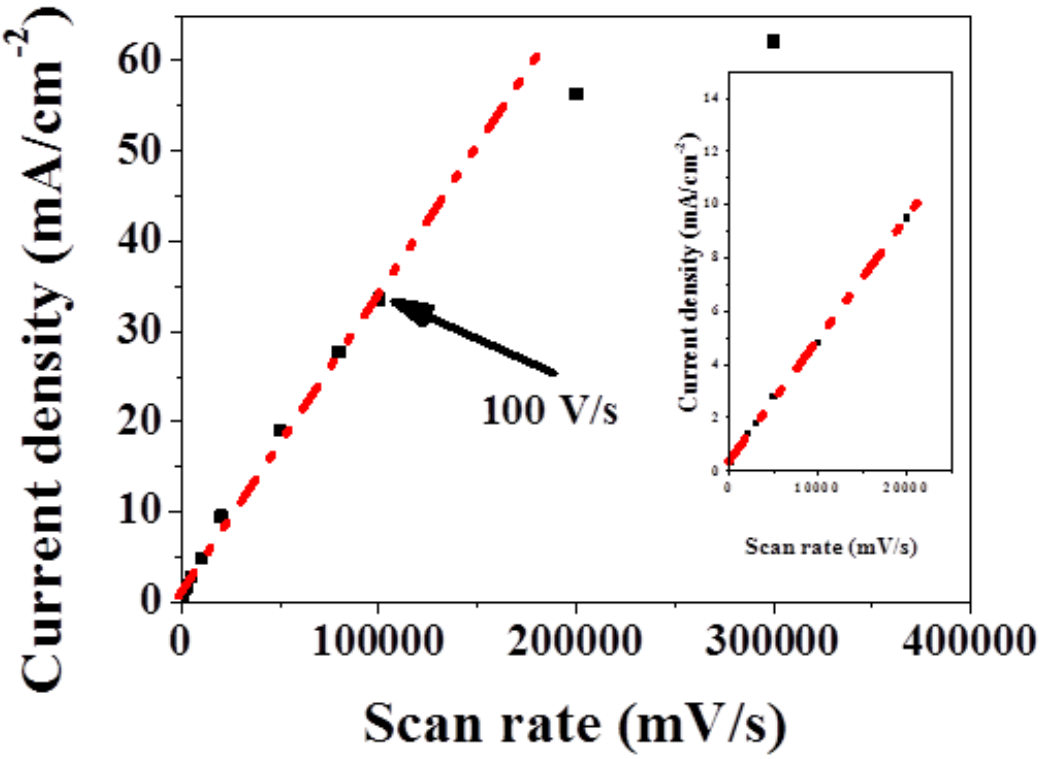

Supplementary Figure 18. Discharge current density *VS*. Scan rate showing linear relationship.

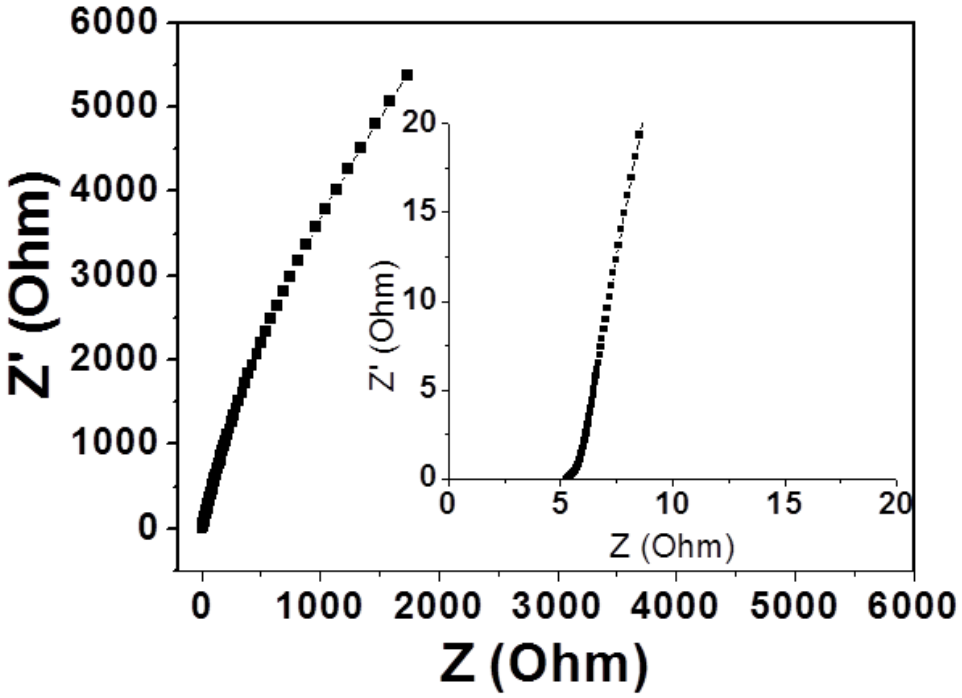

Supplementary Figure 19. Electrochemical Impedance Spectroscopy of MoS_2-S in 0.5 M H2SO4 solution.

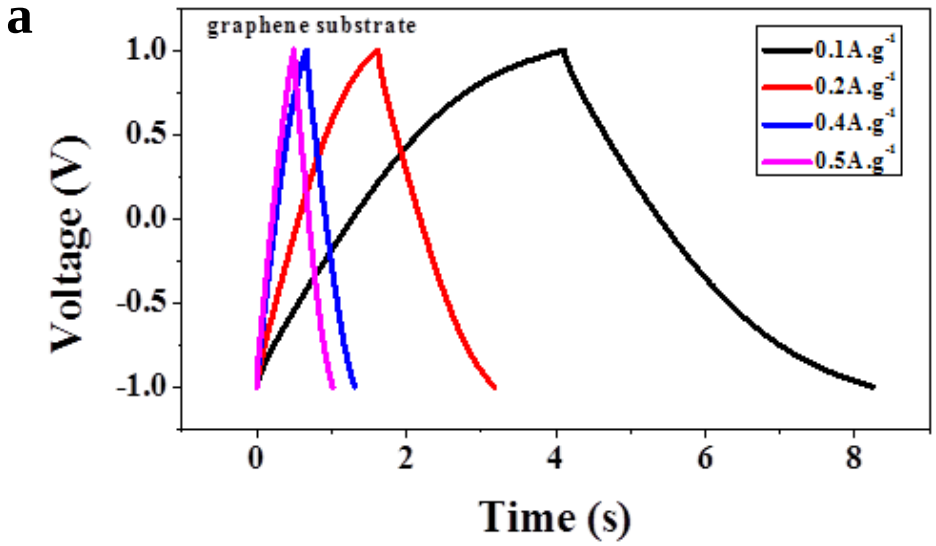

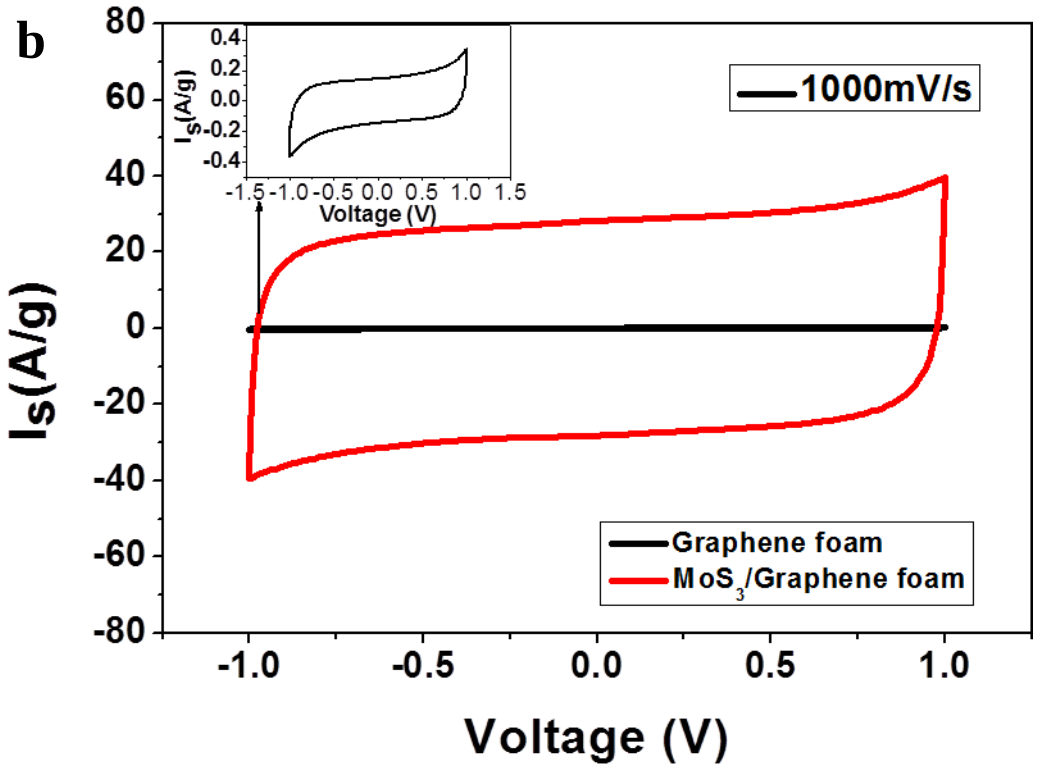

Supplementary Figure 20. Galvanostic charge/discharge curves of graphene foam and CV curve. (a)Charge and discharge curve of graphene foam. (b) Comparison CV curve of graphene foam and MoS_2-S under same 1000mV/s scan rate.

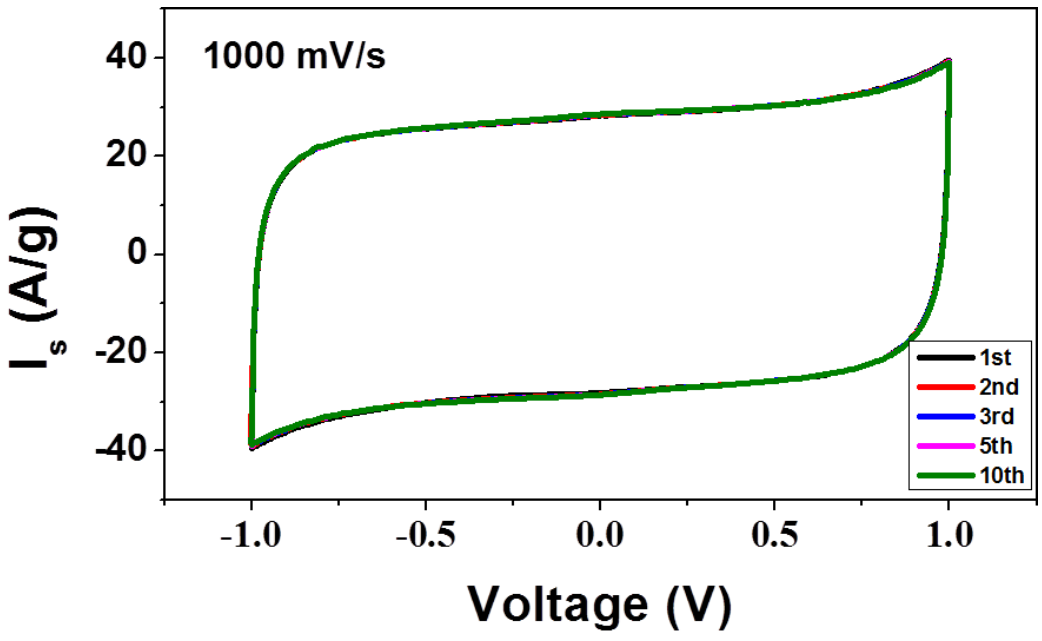

Supplementary Figure 21. CV curves of MoS_2-S working electrode in EMIM BF4/AC at 1000mV/s scan rate. We found from the first 10 cycles showing the quick CV response as the very first cycle. Even though the viscosity of organic electrolyte is bigger than aqueous electrolyte, the kinetic was considered to be sluggish, but initial CV curve show that the good electric conductivity overwhelms ionic conductivity which is consistent with MoS_2-S inherent good electric conductivity.

Discussions on interpretation of computational results

I. Computations in Figure 1 in the main text.

1) The out-of-plane pressure components in the simulation domain from calculation are: 0.0989 GPa for optimized structure in Figure 1(c), -0.0516 GPa for optimized structure Figure 1(d). Calculation wise, these are tiny numbers. They suggest that these optimized structures are close to energetic favorable state at almost zero pressure.
2) The thin lines in the top two rows of Figure 1 show the boundary of simulation domain, and the simulation domain has periodical boundary conditions along three directions (e.g.,x, y, z). The simulations in Figure 1 do not involve explicit control on the external hydrostatic pressure. The purpose of Figure 1 is to demonstrate the template effect without applying significant hydrostatic pressure, and we would like to achieve better comparison between cases by enforcing same simulation setup as much as possible. The Mo-Mo in-plane distance is fixed to be 0.32 nm for Figure 1(b-d), while the S-S in-plane distance is fixed to be 0.32 nm for Figure 1(a). In other words, the simulation domain sizes along the in-plane directions are fixed and controlled to be the same. There is huge vacuum space for structures in Figure 1(a-c). The vacuum space can be generally considered as the maximum-sized Cuboid of space in the simulation domain that contains no atoms. Therefore, the structures in Figure 1(a-c) are effectively monolayers (or slabs). There is no vacuum space treatment for structures in Figure 1(d).
3) The simulations in Figure 1(b-c) are structure relaxation based on Conjugate-gradients optimization, with the constraint that Mo-Mo in-plane distance is fixed as 0.32 nm. While the Mo-Mo in-plane distance is fixed and not allowed to vary during the structure relaxation, the positions of S atoms are optimized towards the minimum energy state. In these cases, the simulation domain size along the out-of-plane direction does not matter since there is huge vacuum space. As for the extra S layers, they will find themselves comfortable not too close to the atoms in MoS_2 in order to avoid the large repulsive forces. Similarly, they also feel the attractive force (e.g. Van der Waals force) from atoms in MoS_2. Therefore, the positions of the atoms in extra S layers are optimized to be in equilibrium among the repulsive forces and attractive forces. The simulations

in Figure 1(d) are also structure relaxation based on Conjugate-gradients optimization, with the constraint that Mo-Mo in-plane distance is fixed as 0.32 nm. However, since there is no vacuum space treatment, the simulation domain size along the out-of-plane direction is optimized during the structure relaxation. It is understandable that too-small domain size along the out-of-plane direction is able to cause large repulsive force (negative, compressive pressure) within the simulation domain. As a result, the structure relaxation would increase the domain size along the out-of-plane direction to reduce the large repulsive force (minimize the magnitude of compressive pressure). Similarly, too-large cell size along the out-of-plane direction is able to cause attractive force (positive, tensile pressure) within the simulation domain which tries to bring the structure together by shrinking the domain. As a result, the structure relaxation would adjust the domain size along the out-of-plane direction to reduce the attractive force (minimize the magnitude of tensile pressure). Therefore, the positions of the atoms in extra S layers and the domain size are varied together during the structure relaxation, in order to reach the equilibrium among the compressive pressure and tensile pressure.

II. Computations in Figure 2 in the main text.

Distinct from the methodology in Figure 1 described above, here the simulations are structure relaxation based on Conjugate-gradients optimization, with the constraint that the simulation domain is in equilibrium with external hydrostatic compressive pressure. All the atoms in the simulation domain are allowed to adjust their position within the simulation domain, and the size of simulation domain is allowed to be changed during the optimization. Therefore, MoS_2 is allowed to deform in-plane. However, as the hydrostatic compressive pressure is applied, there is no in-plane tensile deformation in the simulation domain. From Figure 2(b) and Figure 2(d), we can see that the in-plane domain size decreases as the compressive pressure increases.

III. The nature of mechanical effect from extra S layer on MoS_2.

1) The extra S layer is causing in-plane compression on the MoS_2. To show this, we have compared the in-plane pressure components for optimized structures as shown in Figure 1(b) and Figure 1(c). The only difference between these two structures is the presence of the additional S layers. Therefore, by comparing the in-plane pressure components of the simulation domain, we are able to gather some information on the influence of the interaction between extra S and MoS_2 on the in-plane pressure. Below, p_xx and p_yy are in-plane pressure components.

    - For structure in Figure 1(b) (no extra S), p_xx= -0.482896 GPa (compressive), p_yy= -0.484338 GPa (compressive);
    - For structure in Figure 1(c) (with extra S), p_xx= 1.2513 GPa (tensile), p_yy= 1.0893 GPa (tensile).

Immediately we can see that there is a transition from compressive in-plane pressure to tensile in-plane pressure in the simulation domain as the extra S layer is added while other factors are kept unchanged. Please noted that the tensile in-plane pressure indicates that the simulation domain wants to shrink in-plane. Therefore, it means that the extra S layer is causing in-plane compression on the MoS_2.

2) At these atomic spacings, the extra S layer itself wants to shrink in-plane. To show this, we present the in-plane pressure of pure S cases as in Figure 1(a). We present further data on a similar set up of Figure 1(a), while considering five S-S in-plane distances (0.29 nm, 0.30 nm, 0.31 nm, 0.32 nm, 0.33 nm) and then compare the in-plane pressures. The results are displayed below.

    - 0.29 nm (S layer only), p_xx= 2.786 GPa (tensile) , p_yy= 2.7893 GPa (tensile)
    - 0.30 nm (S layer only), p_xx= 2.8948 GPa (tensile), p_yy= 2.8977 GPa (tensile)
    - 0.31 nm (S layer only), p_xx= 2.8668 GPa (tensile), p_yy= 2.8676 GPa (tensile)
    - 0.32 nm (S layer only), p_xx= 2.7719 GPa (tensile), p_yy= 2.763 GPa (tensile)
    - 0.33 nm (S layer only), p_xx= 2.5922 GPa (tensile), p_yy= 2.59825 GPa (tensile)

    The increasing-decreasing trend as a function of inter atomic distance is understandable similar to the general understanding of Van der Waals attraction force as a function of distance.

    We can see that as the S-S in-plane distance ranges from 0.29 nm to 0.33 nm, there are always tensile in-plane pressures in the simulation domain. Please be noted that the tensile in-plane pressure indicates that the simulation domain wants to shrink in-plane. Therefore, such extra S layer wants to shrink in-plane.

    Then consider the presence of extra S layers on MoS_2. If the driving force for the extra S layer to shrink dominates the entire simulation domain, then there will be in-plane tensile pressure in the simulation domain. This explains the transition from compressive in-plane pressure to tensile in-plane pressure in the simulation domain as the extra S layer is added while other factors are kept unchanged.

3) The driving force for the extra S layer to shrink in-plane is NOT always dominating. To show a case where the driving force for the extra S layer to shrink in-plane is not dominating the entire simulation domain, we present further data on a similar set up of Figure 1(c), while considering two additional Mo-Mo in-plane distances (0.29 nm, 0.30 nm), and then compare the in-plane

pressures. Including the existing data of Figure 1(c) (Mo-Mo in-plane distance 0.32 nm), the results are displayed below.

- Optimized structure with Mo-Mo in-plane distance 0.29 nm, p_xx= -6.2206 GPa (compressive), p_yy= -6.3486 GPa (compressive);
- Optimized structure with Mo-Mo in-plane distance 0.30 nm, p_xx= -2.9967 GPa (compressive), p_yy= -3.1335 GPa (compressive);
- Optimized structure with Mo-Mo in-plane distance 0.32 nm (the existing data of Figure 1(c)), p_xx= 1.2513 GPa (tensile), p_yy= 1.0893 GPa (tensile);

Immediately we can see that at smaller Mo-Mo in-plane distance such as 0.29 nm and 0.30 nm, there are compressive in-plane pressures in the simulation domain. Please be noted that the compressive in-plane pressure indicates that the simulation domain wants to expand in-plane. Such cases demonstrate that driving force for the extra S layer to shrink is not always dominating if the MoS_2 are compressed in-plane too much and therefore the driving force for MoS_2 to expand in-plane is dominating.